Journal of Materials Chemistry B

Accepted Manuscript

ROYAL SOCIETY OF CHEMISTRY

www.rsc.org/materialsB

Poly(acrylic acid)-Chitosan-Silica Hydrogel Carrying Platelet Gel for Bone Defect Repair

Yiu-Jiuan Lin[1], Feng-Chien Hsu[2], Chih-Wei Chou[3], Te-Hsing Wu[4], and Hong-Ru Lin[2,*]

[1]Department of Nursing
Chung Hwa University of Medical Technology, Tainan 717, Taiwan
[2]Department of Chemical and Materials Engineering
Southern Taiwan University of Science and Technology, Tainan 710, Taiwan
[3]Department of Cosmeceutics, College of Pharmacy
China Medical University, Taichung 404, Taiwan
[4]Institute of Nuclear Energy Research, Taoyuan 32546, Taiwan

*Corresponding author: Hong-Ru Lin, Professor, Department of Chemical and Materials Engineering, Southern Taiwan University of Science and Technology, Tainan 710, Taiwan
Tel: +886-6-253-3131; Fax: +886-6-242-5741; E-mail address: hrlin@mail.stust.edu.tw (H. R. Lin)

Abstract

Most of hydrogels derived from either natural or synthetic sources suffer from lack of mechanical strength. In this study, high strength poly(acrylic acid)-chitosan-silica (PAA-Ch-Si) hydrogels were prepared by UV polymerization for tissue engineering application. The compressive strength up to 42 MPa can be achieved by the formation of an interpenetrating network (IPN) structure between PAA and chitosan with nano-silica as filler. The preliminary cell culture of osteoblast cells (7F2) on PAA-Ch-Si hydrogels indicates good biological safety. The growth factor (platelet glue) is fast and completely released from PAA-Ch-Si hydrogel scaffold within 620 min. The scaffold starts to degrade after eight months in vitro. The histological examination demonstrates that the hydrogel incorporated with growth factor and osteoblast cells can promote the cell migration. All of these results illustrate that PAA-Ch-Si hydrogels are beneficial for tissue engineering application and can be used as scaffold for bone defect repair.

1. Introduction

Localized bone defects caused by traumatic conditions, congenital causes or orthognathic surgery need reconstruction for functional and aesthetic purposes.

Autogenous, allogeneic and xenogeneic bone grafts and alloplastic bone substitutes, have all been used for clinical reconstruction; however, they have their own merits and shortcomings [1, 2]. Tissue engineering offers an alternate way to meet the tremendous need for organs and tissues [3-6]. In general, tissue engineering seeks to fabricate living replacement parts for the body [7, 8]. For this purpose, tissue engineering relies on a scaffold that can be used as a space filling material and for cell and therapeutic agent delivery [9]. In the most cases, polymeric scaffolds are used for mechanical support, tissue guidance, or as carriers for growth factors to accelerate bone healing when placed in vivo.

Due to their hydrophilic and cross-linkable properties, hydrogels can absorb a large amount of water and maintain a three-dimensional network structure. The strong water absorbance and rubbery nature of hydrogels resemble those of natural tissues; therefore, hydrogels can be applied as scaffolds for repairing and regenerating a wide variety of tissues and organs. Additionally, it also can be used as carrier for growth factor and cells. Hydrogels for biomedical applications can be prepared by using a wide range of natural and synthetic polymers [10-12]; among them, chitosan and poly(acrylic acid) (PAA) are widely used to prepare hydrogels. Studies have demonstrated that chitosan has excellent biocompatibility [13, 14] and enzymatic biodegradability [15]. More importantly, chitosan can be chemically modified through its amino and/or hydroxyl groups to form complexes and introduce desired functionalities for specific purposes [16, 17]. Many studies have been conducted on the design and fabrication of chitosan-based hybrid systems in order to achieve improved mechanical properties as well as improved biological performances [18, 19]. Poly(acrylic acid) (PAA) is a typical pH-responsive polyelectrolyte, which forms gel when pH is greater than its pKa (4.75) [20, 21]. The use of PAA hydrogel scaffolds in tissue-engineering applications is limited owing to their weak mechanical properties, which limits their further application as templates for tissue regeneration [13, 14].

Platelet-rich plasma (PRP) is defined as an autologous concentration of platelets in a small volume of plasma and has been used to accelerate the healing of both soft tissues and bones [22]. It can promote intensive stimulation of healing through releasing growth factors that are actively secreted by the platelets [23]. These growth factors include three isomers of platelet-derived growth factors (PDGF αα, PDGF ββ and PDGF αβ), two of the numerous types of transforming growth factor beta (TGF β1 and TGF β2), vascular endothelial growth factor (VEGF) and epithelial growth factor (EGF). PRP also has three blood proteins that are known to act as cell adhesion molecules for osteoinduction, bone matrix, connective tissue and epithelial migration [22]. These cell adhesion molecules are fibrin itself, fibronectin and

vitronectin [22]. Platelet gel obtained by mixing a PRP with thrombin [24] has received much attention in bone defect repair. However, platelet gel is weak, gelatin-like fragile biomaterial which is unsuitable to hold bone substitute in a convenient manner for the repair of large bone defects, such as cranial repair [24]. Therefore, in this study, hydrogel was used as a carrier to carry growth factor for bone defect repair.

In this study, in order to overcome the limitations, UV polymerization was used to prepare hydrogels that have an interpenetrating polymer network (IPN) composed of PAA and chitosan. It is expected that the interpenetration of the two networks can provide considerably higher mechanical strength with respect to the homo-polymer network [25]. Nano-silica (colloidal, 20–30 nm) was also incorporated inside the hydrogels to improve their mechanical properties. The physical characterization of the prepared hydrogels, including the swelling ratio, water content and mechanical properties were investigated. In addition, a preliminary cell culture of osteoblasts (7F2) on these hydrogels was undertaken to examine their biocompatibility. 7F2 cells is a spontaneously immortalized cell line isolated from mouse bone marrow (the source of mesenchymal stem cells, MSCs) and appears to correspond to mature osteoblasts because they express alkaline phosphatase, secrete type I collagen, show a significant cyclic adenosine monophosphate response to parathyroid hormone, secrete osteocalcin, and mineralize extensively [26]. They are osteoblast-like bone precursor cells which play a major role in new bone formation. The biological response of primary culture of MSCs may be closer to an in vivo situation than the one obtained with cell lines; however, unlike primary culture of MSCs, the use of 7F2 cell line has more consistent osteoblastic behavior and less difficult to control cellular healthy (such as lower risk of contamination and the problem of passage in primary culture). The histological examinations were obtained by observing the Hematoxylin-eosin (HE) and Masson's Trichrome (MT) stains.

2. Materials and method

2.1 Materials

Acrylic acid (AAc) was purchased from Merck (Germany), N,N'–methylenebisacrylamide (NMBA) from Fluka (USA), and ammonium peroxodisulfate (APS) from Wako (Japan). O-carboxymethyl chitosan (CS, degree of deacetylation 85%; viscosity: 5 CPS, 20℃; 50~60 kDa) was supplied by Charming & Beauty (Taiwan) and glutaraldehyde (GA) from Merck (Germany). Silica (Si, colloidal, 20–30 nm) was supplied by Sunstar Chemical (Taiwan). All other chemicals and reagents used were of analytical grade.

2.2 Preparation of PAA-Based Hydrogels

A series of PAA-based hydrogels were prepared by UV polymerization. To prepare PAA hydrogels, 24.71 ml acrylic acid (AAc) solution was added into 40 ml distilled water and stirred continuously; then, 0.062 g cross-linking agent (NMBA), 0.091 g initiator (APS) and 100 μl of cross-linking agent (GA) were added into the above solution and stirred continuously until they were completely dissolved. The solution of the mixture was then injected into a circular glass mold with a diameter of 1.5 cm. Subsequently, the glass mold was exposed to UV light (2200 W, MHIOEBS, Hexman, Taiwan) for an hour. After polymerization, the gel was immersed into a large amount of double-distilled water for three days in order to remove the unreacted monomer. During the washing cycle, the distilled water was regularly replaced with fresh water. To prepare PAA-Ch and PAA-Ch-Si hydrogels, the desired amount of chitosan (4 g) or silica aqueous solution (50 ml 9% (v/v)) was added to the above aqueous solution and the rest of the procedure was the same as above.

2.3 FT-IR Spectrum Analysis

The dried hydrogels were ground with potassium bromide in the ratio 1:99 in an agate mortar, and they were pressed to a disk. The Fourier transform infrared spectroscopy (FT-IR) spectra were obtained by using a Perkin Elmer infrared spectrometer (Spectrum One, USA) for investigating the UV polymerization reaction.

2.4 Interior morphology observation of hydrogels

The prepared hydrogels were immersed in phosphate buffered saline (PBS) at 25 ℃ until equilibrium was attained. The swollen hydrogels were then frozen at -40℃ overnight prior to being subjected to lyophilization (FD-5N, EYELA, Japan). Specimens of the freeze-dried hydrogels were fractured carefully and their interior morphology was observed by scanning electron microscopy (SEM, S-3000N, Hitachi, Japan). Before conducting SEM observations, the specimens of the hydrogel was fixed on aluminum stubs and coated with gold for 60 s.

2.5 Compression Test

The compression measurements were performed on a swollen hydrogel in PBS at 25 ℃ by using a universal material tester (AG-IS, Shimadzu, Japan) at a compression rate of 10 mm/min. The data were used to calculate the shear modulus (G) and cross-linking density (ρ_x) [27] using equations (1) and (2):

$$\tau = F/A = -G(\lambda - \lambda^{-2}), \quad (1)$$

$$\rho_x = G v_2^{-1/3}/RT, \quad (2)$$

where τ denotes the compression stress, F the compression load, A the

cross-sectional area of the swollen hydrogels and λ the compression strain (L/L_o). For low strains, a plot of the shear stress versus $-(\lambda - \lambda^{-2})$ would yield a straight line whose slope is the shear modulus. v_2 denotes the volume ratio of the hydrogel at absolute temperature T and R is the gas constant. Three specimens were measured for each gel.

2.6 Degradation test

Degradation of the prepared hydrogels in PBS was studied at different intervals of time. The hydrogel was soaked in PBS under 25℃ to let it completely swells; after been frozen under -40℃, dewater it with a freeze-dryer (FD-5N, EYELA, Japan) and then weigh it. Subsequently, the hydrogel was immersed in PBS at 37℃. The hydrogel was periodically removed to a setting under -40℃ for freezing, and finally freeze-dry it, weigh it and record its weight. Based on the variation of its weight, it can be determined whether it degrades after long-time soaking in PBS.

2.7 Cell Culture

Before examining the biological response of these hydrogels, they were subjected to washing cycles at 25℃ under deionized water for three times in order to eliminate the residual monomers that are potentially toxic. The specimens of the freeze-dried hydrogels were fractured carefully without destroying the interior morphology of the hydrogels. The hydrogel materials were cut opportunely to fit into 96-well plates. These materials were treated twice with PBS containing penicillin, streptomycin and fungizone for 24 h at 37℃ in a 5% CO_2 humidified atmosphere. 7F2 osteoblasts were employed to evaluate the ability of the hydrogels to promote cell adhesion and proliferation. Cells of the third passage were used in the all the experiments. The cells were seeded in wells containing the materials at a density of 1×10^5 cell/ml. The materials were then equilibrated at DMEM and incubated at 37℃ in a 5% CO_2 humidified atmosphere. The medium was changed daily and the samples were withdrawn for further analyses after desired period of seeding time.

2.8 MTS Test

The cell vitality and proliferation in all the experiments were evaluated by means of the MTS assay. This method is based on the reduction of the tetrazolium ring of the inner salt, 3-(4,5-dimethylthiazol-2-yl)-5-(3-carboxymethoxyphenyl)-2-(4-sulfophenyl)-2H-tetrazolium (MTS), by the mitochondrial dehydrogenase of living cells. The reaction yields blue formazan crystals that can be promptly solubilized for spectrophotometric quantification. The amount of formazan produced is proportional to the viable cell

number. 20 ml MTS was added into the samples after seeding for the desired period of time. The medium was then withdrawn after three hours and analyzed by using an ELISA reader (Anthos 2010, Tecan Sunrise, Switzerland) at 490 nm.

2.9 The releasing of platelet gel

Firstly, 0.5 ml thrombin was added to 19 ml PBS; after properly mixing, 0.5 ml platelet was added to it and mixed properly. The hydrogel scaffold was then immersed in the platelet gel solution for adsorption under 4℃ and it was removed from the solution after swelling equilibrium was obtained. Subsequently, it was placed in PBS without platelet gel for drug releasing. At each time point, 100 µl of releasing medium was taken and placed in a 96-welled plate. Measurement of the level of PDGF αα was then conducted by ELISA (Bio-Tek power wave XS, USA) at a wavelength of 492 nm.

2.10 Animal studies

This study uses mature rats which weigh 250-300g. All animal experiments were performed in compliance with guidelines approved by the Animal Use and Care Administrative Advisory Committee at the Southern Taiwan University of Science and Technology, Tainan, Taiwan. Since human cartilage exists in bone, the mode of bony impairment is selected and sodium pentobarbital (50 mg/ml) is injected at lateral thigh to form 3 mm of bony impairment. For the negative control group, the bony impairment is left un-rebuilt, but stanch bleeding with cotton merely. For the positive control group, the bony impairment is rebuilt with hydrogel. For the experimental group, one is rebuilt with hydrogel and osteocyte. The other is rebuilt with hydrogel, osteocyte, and platelet gel. Observation is conducted at several time points, 1, 2, 4, and 8 weeks after the surgery. Also it is observed whether inflammation and elimination occur in the implant. At each time point, the animals which are injected excessive sodium pentobarbital should be sacrificed, and the implants and peripheral bone (5-6 mm) are extracted for observation and assessment by HE and MT stains.

2.11 Statistical analysis

Results are given as means SD. Statistical analysis was performed using Student's t test. Multiple comparisons were done using one way ANOVA and Dunnett's test. Statistical significance was set at $P < 0.05$.

3. Results and Discussion

3.1 Structure investigation of PAA-Ch-Si hydrogel

In this study, in order to improve mechanical properties of hydrogel, UV

polymerization was used to prepare hydrogel that has an interpenetrating polymer network (IPN) composed of PAA and chitosan. Nano-silica (Si) was also incorporated inside the hydrogel to improve its mechanical properties. This research uses PAA as substrate and irradiates it with UV to form hydrogel through free radical addition polymerization [28]. UV breaks the bonds with its high energy to polymerize hydrogel, which largely shorten the time required, reduces toxicity, and speeds up polymerization. When mixing AAc, NMBA, and APS, free radical polymerization is induced by irradiation of UV and they polymerize into PAA. NMBA as crosslinking agent serves to bridge between PAA molecular chains and form network. The literature indicates that polymer network formed by free radical polymerization is always accompanied by void formation in its microstructure [29]. When nano-silica disperses in AAc solution during polymerization, it generates hydrogen bonding between PAA and nano-silica simultaneously [30]. Furthermore, since silica has nano-level particle size and behaves agglomeration, it might enter the void in the PAA structure during polymerization. Once the hydrogen bonding between silica and PAA has formed, they will form a denser network in the void.

On the other hand, chitosan forms its own network under acid environment. The internal and external crosslinking forms through the condensation reaction between aldehyde group of GA and amino group of chitosan, which strengthens the mechanical properties of chitosan network [31]. The gelation mechanism of this work is caused by the intertwisting between networks of PAA and chitosan through electrostatic Coulomb force, since PAA has negative charge, while chitosan has positive [28]. To clearly express the mechanism of the overall PAA-Ch-Si hydrogel formation, it is schematized as Figure 1, where the solid line is network of PAA and dotted line is that of chitosan, which intertwist with each other, while nano-silica enters the void in the PAA structure and forms hydrogen bond with PAA. As a result, polymerization by irradiation of UV creates a full-IPN structure. This paper further subjects the hydrogel polymerized here to investigation of ties of matter and test of biocompatibility, in order to determine whether this hydrogel is applicable to serve as carrier for repairing impaired bone tissue.

3.2 IR spectra of PAA-Ch-Si hydrogels

IR spectra of PAA, PAA-Ch, PAA-Si and PAA-Ch-Si are shown Figure 2 and the corresponding functional groups and their absorption wavenumbers are listed in Table 1. The transmittance bands at 1463 cm^{-1}, 1714 cm^{-1}, and 3452 cm^{-1} are ascribed to COO^-, C=O, and OH of the PAA hydrogel, respectively. In PAA-Ch hydrogel, the characteristic absorption peak of amide II from chitosan caused by the C-N stretching and C-N-H bending shifts to 1410 cm^{-1}. The shifting is probably caused by

the intertwisting between PAA and chitosan networks via electrostatic force [32]. The C=O from PAA also shifts to 1729 cm^{-1} due to the network interactions between PAA and chitosan. Absorption peaks observed from PAA-Si hydrogel due to Si–O–Si stretching of silica occurs at 1120 cm^{-1} and C=O from PAA shifts to 1729 cm^{-1}. These characteristic absorption peaks are all observed in PAA-Ch-Si hydrogel excepting the Si–O–Si stretching of silica slightly shifts to 1051 cm^{-1} and C=O from PAA shifts to 1669 cm^{-1}, probably caused by the hydrogen bonds formation between PAA and silica. This provides evidence for the successful preparation of PAA-Ch-Si hydrogel through UV polymerization.

3.3 Interior morphology of PAA-Ch-Si hydrogels

Hydrogel being applied to repairing impaired bone should have good void connectivity to insure it will allow body fluid and other water-soluble materials to pass through after being applied to human body. Also, it should be able to release the drug it carries rapidly to ensure rapid efficacy of treatment. The interior morphology of the lyophilized hydrogel is observed with SEM and shown in Figure 3. All the hydrogels show interconnected pore structure with variation of cell-struct thickness. The average void diameter with narrow distribution of both PAA (16.7 μm) and PAA-Ch (14.1 μm) hydrogel is slight larger than that of PAA-Si (13.5 μm) and PAA-Ch-Si (12.4 μm). The cause may be that addition of nano-silica makes them denser and that agglomeration of nano-silica enhances formation of denser network. It is clear that cell-struct thickness of PAA-Ch-Si hydrogel (Fig. 3 (d)) is the largest among others, which is expected to have the largest mechanical strength among other hydrogels. The void structures of these four hydrogels are all helpful for, after being implanted to impaired bone tissue, absorbing body fluid to maintain a certain water content and allowing nutrition to pass through.

3.4 Mechanical properties of PAA-Ch-Si hydrogels

To prove whether the hydrogel carrier prepared by this study has certain strength to resist foreign stress, the compressing test was conducted. It is clear from Table 2 that PAA hydrogel has compressive strength about 5 MPa, while that of PAA-Ch hydrogel added with chitosan increases to 6.3 MPa and PAA-Si hydrogel polymerized by adding silica as filler increases to 8.9 MPa. On the other hand, PAA-Ch-Si hydrogel has compressive strength as high as 42MPa. It is speculated that such significant difference ($p<0.001$ compared to PAA, PAA-Ch, and PAA-Si hydrogels)is caused by intertwisting between PAA network and the network formed by chitosan itself, and that the filler silica might has dispersed into the voids inside PAA network which makes denser void network which is able to resist more foreign

stress. Thus the overall compressive strength increases. Employing such hydrogel carrier to repair cartilage can meet the load required by knee joint cartilage, 2-5 MPa [28]. It is a pity that such hydrogel cannot reach the required load, 150 MPa [33], if it is used to repair impaired bone; however, bone has better recovery ability but requires longer time, the hydrogel can serve as carrier for bone and adsorb growth factor to shorten time of self-repair.

Entering the data yielded by compressive test to equations 1 and 2 will generate cross-linking density which is compiled as Table 2. The cross-linking density of PAA hydrogel is the lowest (0.195×10^{-5} mole/cm^3), and that increases slightly (0.204×10^{-5} mole/cm^3) when PAA hydrogel is added by chitosan, but that increases to about 0.764×10^{-5} mole/cm^3 when the filler silica is added to the PAA hydrogel. However, when both chitosan and silica were incorporated (i. e. PAA-Ch-Si hydrogel), a cross-linking density as high as 2.293×10^{-5} mole/cm^3 can be obtained, which is significant higher than the other three values ($p<0.001$). The main cause is the polymerization driven by UV irradiation which forms intertwisting between PAA network and the network that chitosan forms by itself. And also the filler silica enters the voids in the PAA network to form hydrogen bonding during its dispersion, which increases density of cross-linking and as a result increases mechanical strength of the hydrogel [34]. The elastic modulus and toughness of PAA-Ch-Si hydrogel are significant higher than the other three hydrogels ($p<0.05$), respectively. In addition, as listed in Table 2, toughness and cross-linking density correspond to compressive strength, that is, the higher toughness and cross-linking density, the higher compressive strength. The cross-linking density is also consistent with elastic modulus, that is, the higher cross-linking density, the higher elastic modulus, and so the better material strength. This validates that the PAA-Ch-Si hydrogel prepared by this study has the potential to resist the stress of impairment in bone tissue.

3.5 Degradation behavior of PAA-Ch-Si hydrogels

In order to figure out whether hydrogel scaffold prepared by this study can be implanted to human body for a long period of time without being degraded, the hydrogel was observed in PBS, 37℃, for eight months. Firstly from its appearance, there is not obvious variation in the first four months but it is significantly softened without degradation during the fifth and sixth months. From Figure 4, it is clear that weight of hydrogels increases with time. The cause may be that the hydrogel absorbs PBS during the soaking and that since the PBS contains some salts which are stored in pores of the hydrogel, they accumulate and their weight increases with time after the hydrogel being treated by lyophilization. An important criterion of a scaffold is to maintain a slow degradation rate to facilitate the growth of tissues. In the seventh

month, the degradation of the hydrogel scaffold starts. The cause is speculated to be gradual hydrolysis of PAA and Chitosan in PBS. Due to the pore structure, water molecules can easily penetrate the polymer network. The water molecules are then easily absorbed to scaffold surface since the presence of hydrolytic groups from PAA and Chitosan. The bonds are subsequently dissociated through the hydrolysis. Consequently, the electrostatic Coulomb force between PAA and Chitosan and the crosslinks among molecules may also be disrupted due to molecular structure collapsing [35, 36]. Among them, PAA-Ch-Si hydrogel degrades most after the seventh month since both polymers, PAA and Chitosan, are involved. Normal bone tissue will enter a period of 3 to 5 days of inflammation after injury. And then 1 to 2 months of repair period follows. In this period, osteoclast and osteoblast in the bone tissue are more active, which lead to osteotylus. The osteotylus is very brittle at its early stage but becomes stronger with time. When the osteotylus disappears gradually, the shape of the skeleton and mechanical strength resumes the state before injury. Although the impaired local may be uneven or unsmooth, it will reshape automatically about one year later and creates the best shape and strength [37]. In sum, this hydrogel scaffold is validated to be covering the repair period of the bone tissue.

3.6 Biological response of PAA-Ch-Si hydrogels

To investigate whether hydrogel scaffold prepared in this study is a material with biocompatibility, the sterilized hydrogel scaffolds were placed in a 96-welled plate to culture bone cell of rats (7F2). Bony cells are cultured on the polystyrene plate as control group and compared with other hydrogels. Figure 5 shows that the first day the cell is implanted to the material, the control group has higher values than hydrogel group because the concentration of hydrogel monomer is higher and the interior of the hydrogel is acid so absorbance is lower. In addition, it is obvious from the data that absorbance values of PAA-Si and PAA-Ch-Si hydrogels, after adding silica, is higher than that of PAA and PAA-Ch hydrogels. The hydrogel added by silica has higher water content than the other two groups, so the hydrogel carrier absorbs more medium than the other two groups too. By continuous renew of medium, the hydrogel scaffold added with Si better neutralizes the acid of the hydrogel than the other two groups. Hence, the data shows that the absorbance values of PAA-Si and PAA-Ch-Si hydrogel scaffolds are higher than that of the other groups. Moreover, the absorbance values detected increase with days, indicating cell livability increases too. The data verifies that the hydrogel produced by this experiment allows cells to adsorb, suggesting it has good biocompatibility.

Besides, for PAA-Si and PAA-Ch-Si scaffolds which have better biocompatibility,

this experiment compares their absorbance when they are incorporated with growth factor (platelet gel) and not incorporated in order to figure out whether stimulation of growth factor increases differentiation of bony cells. Figure 6 illustrates that two groups of hydrogel scaffolds added with growth factor on the 56th day have better cell absorbance than other hydrogel scaffolds which are not added with growth factor. It is expected that the difference in MTS data between scaffold and scaffold/platelet gel is more pronounced at earlier time points, since the platelet gel is found to release completely from the scaffold within 11 hours as shown below. This result suggests that addition of growth factor is helpful for differentiation and proliferation of bony cells.

3.7 Release of platelet gel from PAA-Ch-Si hydrogels

The release of platelet gel from PAA-Ch-Si hydrogels was basically measured from the level of PDGF αα at a wavelength of 492 nm. Figure 7 shows the mass remaining of platelet glue release (%) at that specific time. After 420 minutes, platelet gel is released from the hydrogel scaffolds rapidly. PAA-Si and PAA-Ch-Si hydrogel scaffolds have faster release rate than the other two groups, which is speculated due to having smaller void diameter and denser structure in these two groups of hydrogels. This is not beneficial for platelet gel to enter the hydrogels, instead they attach to surface of the scaffolds. Besides, since platelet has function in hemoglutination, and might obstruct in the voids and so coagulate, inhibiting huge amount of platelet gel from entering the hydrogel but attach to the hydrogel surface. As a result, all these four groups of hydrogels have large amount of release after 420 minutes and release completely within 620 min. PRP works by the degranulation of the α granules in platelets, which contain the synthesized and prepackaged growth factors. When bone tissue is impaired, fracture for example, hemoglutination begins. As the clotting process activates the platelets, the growth factors are secreted from the cell through the cell membrane. The secreted growth factors immediately bind to the external surface of cell membranes of cells in the wound by transmembrane receptors. These transmembrane receptors in turn induce an activation of an endogenous internal signal protein, which causes the expression of a normal gene sequence of the cell such as cellular proliferation, matrix formation, osteoid production, collagen synthesis, etc. [22]. A couple of days later, angiogenesis and fibroblasts begin to grow, and then weave-like bone and cartilage are generated. Several months later, the bone is recovered completely [37]. Therefore, rapid release of growth factor stimulates cells' fast proliferation and differentiation, which contributes to shortening the time required by bone recovery.

3.8 Animal studies

To prove that PAA-Ch-Si hydrogel scaffold has good repair efficacy through histological observation, the animal studies refer the bone with 1-8 weeks of impairment to histopathological observation. Figure 8 displays through HE stain that the impaired local heals even better with recovery time. PAA-Ch-Si hydrogel scaffold groups for example, shown as Figure 8 (e)-(h), some cells involved with bony recovery on the local of bony impairment moves to osteotylus in the first week, shown as Figure 8 (e). In the second week, cells moving to the osteotylus increases, shown as Figure 8 (f). In the fourth week, not only the cells continue to increase significantly, newly generated bony tissue appears, shown as local pointed by the solid line arrow in Figure 8 (h). In combination of osteoblasts or simultaneously growth factor, the PAA-Ch-Si hydrogel scaffold group also has similar variations, shown as Figure 8 (i)-(p). On the contrary, although the control group has similar variation, the cells moving to the osteotylus in the first week are dispersed and sparse, shown as Figure 8 (a). In the eighth week, although newly generated bony tissue appears, it is not complete however, shown as Figure 8 (d). From Figure 8 we can see that the hydrogel scaffolds group added by osteoblasts and the other group added by both osteoblasts and growth factor exert better repair to the bony impairment than does control group. Since PAA-Ch-Si hydrogel scaffold has voids that is beneficial for migration and fixation of cells, so more cells can be attracted and migrate to participate bone repair, for example fibroblasts, osteoblasts, and vascular endotheliocytes. Of which, PAA-Ch-Si hydrogel scaffold group added by osteoblasts is better than the group with merely scaffold and the control group, because the osteoblasts added to the PAA-Ch-Si hydrogel scaffold which is then implanted to rat's impaired local begins to proliferate and differentiate, which is beneficial to bony recovery. Fostering osteoblasts on the PAA-Ch-Si hydrogel scaffold and adding growth factor can better stimulate proliferation, migration, and differentiation of cells, and even attract more cells to join the recovery, so contribute to better recovery effect. Therefore, by inclusion of cell therapy, the tissue-engineered construct may be able to survive, restore normal function, e.g. biochemistry and both mechanical and structural integrity, and integrate with the surrounding tissues.

In the recovery process of the impaired bone, not only large amount of fibroblasts, osteoblasts, osteoclasts, and vascular endotheliocytes are required for the recovery but also aids from large amount of extracellular mesenchyme such as collagen fiber. This experiment employs MT stain to observe production of collagen fiber. Figure 9 is MT stain of PAA-Ch-Si hydrogel series. By magnification of 40X, the bony impairment is visible. The stains of collagen fiber (blue) in hydrogel scaffold group, hydrogel scaffold added with osteoblasts group, and that added with both

osteoblasts and growth factor are all more obvious than that of the control group. Under 400X magnification it is observed that the impaired locals under repair in three groups of hydrogel scaffolds have more collagen fiber than that of the control group, of which the hydrogel scaffold added with osteoblasts has more than the pure hydrogel scaffold group. When osteoblasts and growth factor are integrated into the hydrogel scaffold, it is expected that the growth factor can stimulates the cells to produce more collagen fiber so as to help recovery of the bony impairment.

4. Conclusions

PAA-Ch-Si hydrogel was successfully prepared by UV irradiation and its ties of matter were characterized, including observation of surface topography, compressive mechanical properties, degradation behavior, and release of growth factor. The cell culture and animal studies on the hydrogels were also conducted. In sum, addition of nano silica makes the void structure of the hydrogel denser because of its agglomeration. Such PAA-Ch-Si hydrogel has mechanical strength about 42 MPa which meets the load required by the cartilage. With respect to cell culture, the absorbance of PAA-Ch-Si hydrogel scaffold increases with days. The cells added with growth factor (platelet gel) are observed to have significantly larger quantity on the 56th day than that without adding growth factor, indicating growth factor simulates the cells to rapidly proliferate. The hydrogel carrying growth factor becomes a rapid release type of hydrogel scaffold. It reaches complete release within 220 minutes. Regarding degradation, the hydrogel scaffold starts to degrade after nearly eight months' observation. In animal experiment, the findings show that each hydrogel scaffold is beneficial for attracting cells, resulting in higher cell density in the bony impaired local compared with that of the control group. The hydrogel scaffold added with both osteoblasts and growth factor is even more beneficial for inducing cell proliferation and differentiation so as to accelerate recovery ability of the impaired local.

5. References

1. A. J. Weiland, T. W. Phillips and M. Randolph, *Plast. Reconstructr. Surg.*, 1984, **74**, 368.
2. L. DeLuca, R. Raszewski, N. Tresser and B. Guyuron, *Plast. Reconstructr. Surg.*, 1997, **99**, 1324.
3. R. Langer and J. P. Vacanti, *Science*, 1993, **260**, 920.
4. J. R. Fuchs, B. A. Nasseri and J. P. Vacanti, *Ann. Thorac. Surg.*, 2001, **72**, 577.
5. L. E. Niklason and R. Langer, *J. Am. Med. Assoc.*, 2001, **285**, 573.
6. U. A. Stock and J. P. Vacanti, *Ann. Rev. Med.*, 2001, **52**, 443.

7. E. Bell , In *Principles of Tissue Engineering*, ed. R. P. Lanza , R. Langer and J. P. Vacanti, San Diego, Academic Press, 2nd edn., 2000, p. xxxv.
8. D. J. Mooney, *Biomaterials*, 2003, **24**, 4337.
9. J. D. Kretlow and L. Klouda, *Adv. Drug. Deliver. Rev.*, 2007, **59**, 263.
10. J. A. Burdick, C. Chung, X. Q. Jia, M. A. Randolph and R. Langer, *Biomacromolecules*, 2005, **6**, 386.
11. S. J. Bryant and K. S. Anseth, *Biomaterials*, 2001, **22**, 619.
12. H. Tan, C. R. Chu, K. A. Payne and K. G. Marra, *Biomaterials*, 2009, **30**, 2499.
13. H. R. Lin and Y. J. Yeh, J. Biomed. Mater. Res. (Appl. Biomater.), 2004, 71B, 52.
14. K. H. Bouhadir and D. J. Mooney, in Methods of Tissue Engineering, ed. A. Atala and R. P. Lanza, Academic Press, New York, NY, 2002, p. 653.
15. K. Tomihata and Y. Ikada, Biomaterials, 1997, 18, 567.
16. H. Sashiwa and S. Aiba, Prog. Polym. Sci., 2004, 29, 887.
17. M. H. Ho, D. M. Wang, H. J. Hsieh, H. C. Liu, T. Y. Hsien, J. Y. Lai, et al., Biomaterials, 2005, 26, 3197
18. A. Oladn and F. F. Azhar, Ceram. Int., 2014, 40, 10061.
19. K. C. Kavya, R. Jayakumar, S. Nair and K. P. Chennazhi, Int. J. Biol. Macromol., 2013, 59, 255.
20. N. M. Ranjha, G. Ayub, S. Naseem and M. T. Ansari, *J. Mater. Sci. Mater. Med.*, 2010, **21**, 2805.
21. T. Hussain, N. M. Ranjha and Y. Shahzad, *Des. Monomers Polym.*, 2011, **14**, 233.
22. R. E. Marx, *J. Oral Maxillofac. Surg.*, 2004, **62**, 489.
23. G. Crovetti , G. Martinelli, M. Issi, M. Barone, M. Guizzardi, B. Campanati, M. Moroni and A. Carabelli, *Transfus. Apher. Sci.*, 2004, **30**, 145.
24. T. M. Chen, J.-C. Tsai and T. Burnouf, *J. Trauma. Inj. Infect. Crit. Care*, 2007, **65**, 1321.
25. J. Zhang and N. A. Peppas, *J. Biomater. Sci. Polymer Edn.*, 2002, **13**, 511.
26. D. L. Thompson, K. D. Lum, S. C. Nygaard, R. E. Kuestner, K. A. Kelly, J. M. Gimble and E. E. Moore, J. Bone Miner. Res., 1998, 13, 195.
27. T. Jiang, W. I. A. Fattah and C. T. Laurencin, *Biomaterials*, 2006, **27**, 4894.
28. H. R. Lin, M. H. Ling and Y. J. Lin, *J. Biomater. Sci. Polymer Edn.*, 2009, **20**, 637.
29. Y. Tanaka, J. P. Gong and Y. Osada, *Prog. Polym. Sci.*, 2005, **30**, 1.
30. X. Shi, S. Xu, J. Lin, S. Feng and J. Wang, *Mater. Lett.*, 2009, **63**, 527.
31. I. Genta, M. Costantini, A. Asti, B. Conti and L. Montanari, *Carbohyd. Polym.*, 1998, **36**, 81.
32. M.A. Khedr, A.I. Waly, A.I. Hafez, H. Ali and H. Gadallah, Australian Journal of Basic and Applied Sciences, 2012, 6, 174.
33. G. Eskitaşcıoğlu, S. Belli and M. Kalkan, *J. Endodont.*, 2002, **28**, 629.

34. K. S. Wilson, K. Zhang and J. M. Antonucci, *Biomaterials*, 2005, **26**, 5095.
35. I. Y. Kim, S. J. Seo, H. S. Moon, M. K. Yoo, I. Y. Park, B. C. Kim and C. S. Cho, *Biotechnol. Adv.*, 2008, **26**, 1.
36. A. F. Bettencourt, C. B. Neves, M. S. de AlmeidabLidia, M. Pinheiro, S. A. e Oliveira, L. P. Lopes and M. F. Castro, *Dent. Mater.*, 2010, **26**, e171.
37. A. L. Schiller and S. L. Teitelbaum, in *Essential Pathology*, ed. E. Rubin, New York, Lippincott Williams and Wilkins, 3rd edn., 2001, p. 667.

Figure captions

Figure 1. Schematic diagram showing mechanism of PAA-Ch-Si hydrogel formation.

Figure 2. IR spectra of PAA, PAA-Ch, PAA-Si and PAA-Ch-Si hydrogels.

Figure 3. Morphology of (a)PAA, (b)PAA-Ch, (c)PAA-Si, and (d)PAA-Ch-Si hydrogels observed by SEM (×500, 60 μm).

Figure 4. Degradation behavior of various hydrogels in simulated body fluid.

Figure 5. MTS test results of hydrogels with different compositions.

Figure 6. MTS test results of PAA-Si and PAA-Ch-Si hydrogel scaffolds and that added with platelet gel.

Figure 7. Platelet gel released from hydrogels with different compositions.

Figure 8. HE stain patterns (40X) of PAA-Ch-Si hydrogel scaffold series observed on different time. The dashed line arrow points the hydrogel, while the solid line arrow points the newly produced bone tissue.

Figure 9. MT stain patterns (40X and 400X) of PAA-Ch-Si hydrogel scaffold series observed in the second week. The dashed line arrow points the hydrogel.

Table 1. The functional groups and their corresponding wavenumbers for PAA, PAA-Ch, PAA-Si, and PAA-Ch-Si hydrogels.

PAA	PAA-Ch	PAA-Si	PAA-Ch-Si	Functional group
1463 cm^{-1}				COO^-
3452 cm^{-1}				OH
1714 cm^{-1}	1729 cm^{-1}	1729 cm^{-1}	1669 cm^{-1}	C=O
	1410 cm^{-1}		1410 cm^{-1}	Amide II
		1120 cm^{-1}	1051 cm^{-1}	Si–O–Si

Table 2. Mechanical properties of hydrogels with different composition.

Hydrogel	Elastic modulus (MPa)	Strength (MPa)	Strain (%)	Toughness (J)	Cross-link density ($X10^{-5}$ mol/cm^3)
PAA	0.91±0.14*	4.94±1.44**	29.33±3.70	0.76±0.08*	0.195±0.047**
PAA-Ch	1.44±0.18*	6.31±0.50**	32.01±1.44*	1.47±0.16*	0.204±0.041**
PAA-Si	1.49±0.16*	8.92±1.22**	25.92±1.43	1.99±0.68*	0.764±0.152**
PAA-Ch-Si	2.50±0.28	42.26±3.63	25.23±0.59	5.23±1.48	2.293±0.060

* P<0.05 as compared to PAA-Ch-Si

** P<0.001 as compared to PAA-Ch-Si

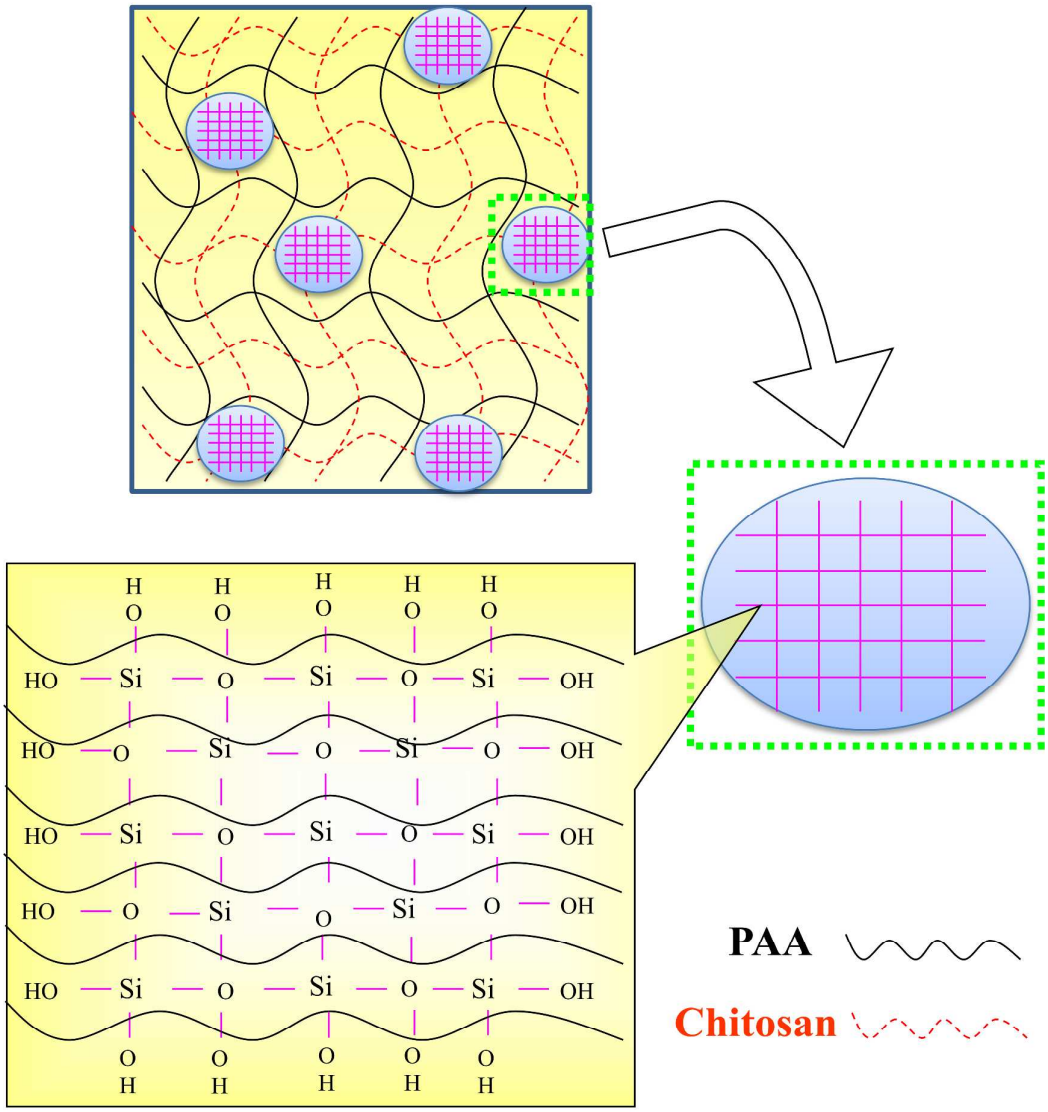

Figure 1. Schematic diagram showing mechanism of PAA-Ch-Si hydrogel formation.

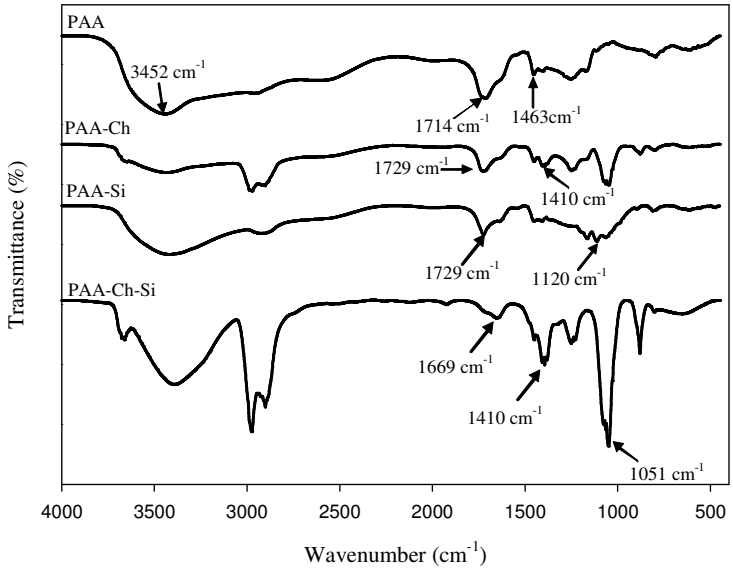

Figure 2. IR spectra of PAA, PAA-Ch, PAA-Si and PAA-Ch-Si hydrogels.

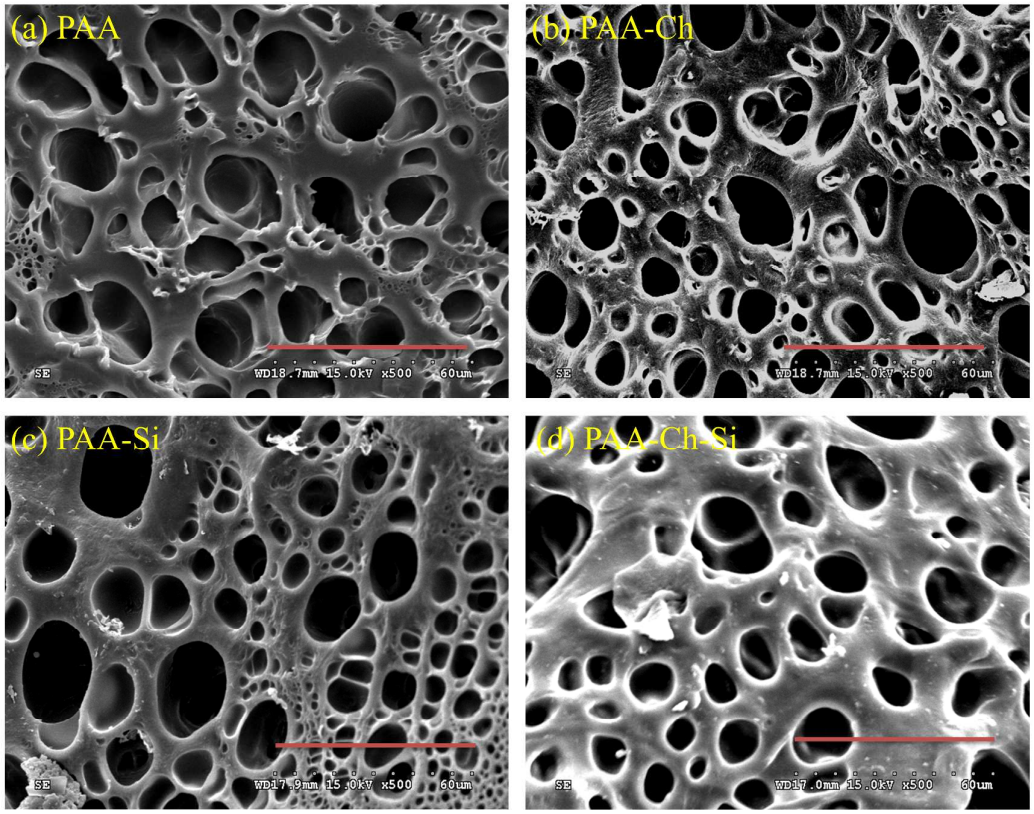

Figure 3. Morphology of (a)PAA, (b)PAA-Ch, (c)PAA-Si, and (d)PAA-Ch-Si hydrogels observed by SEM (×500, 60 μm).

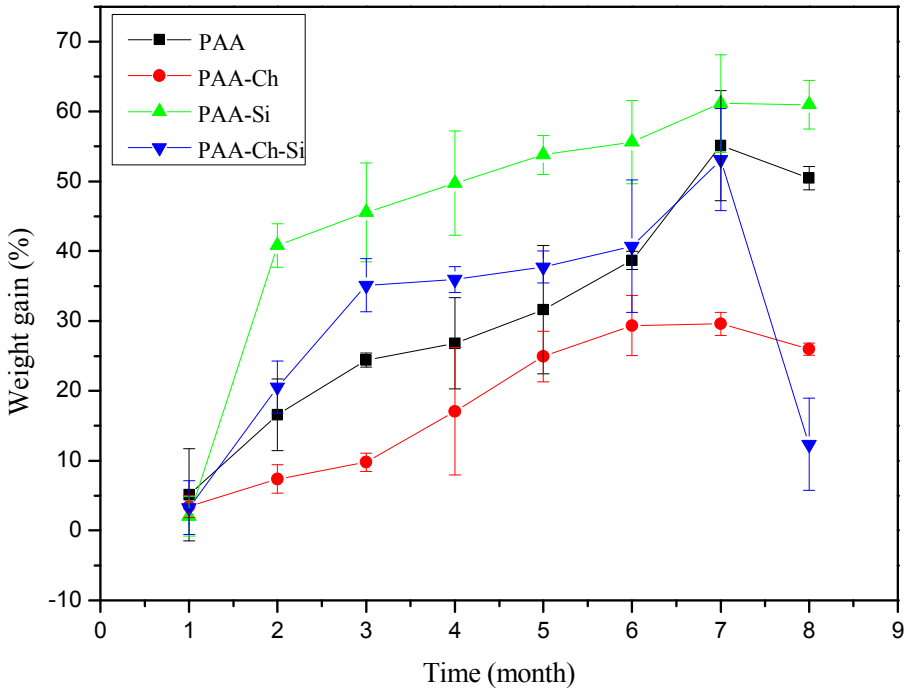

Figure 4. Degradation behavior of various hydrogels in PBS.

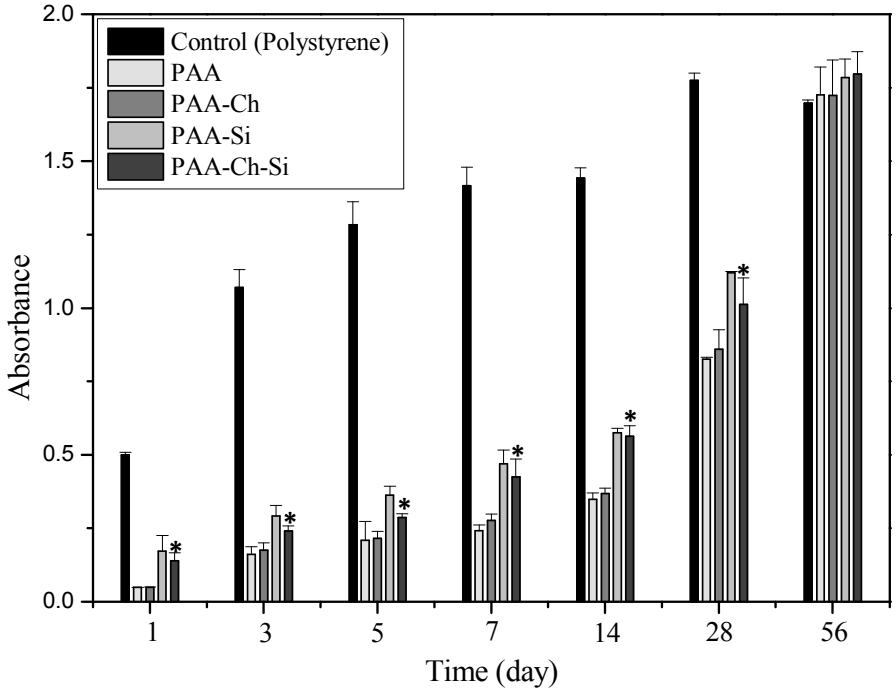

Figure 5. MTS test results of hydrogels with different compositions (*P < 0.05 as compared PAA-Ch-Si to control).

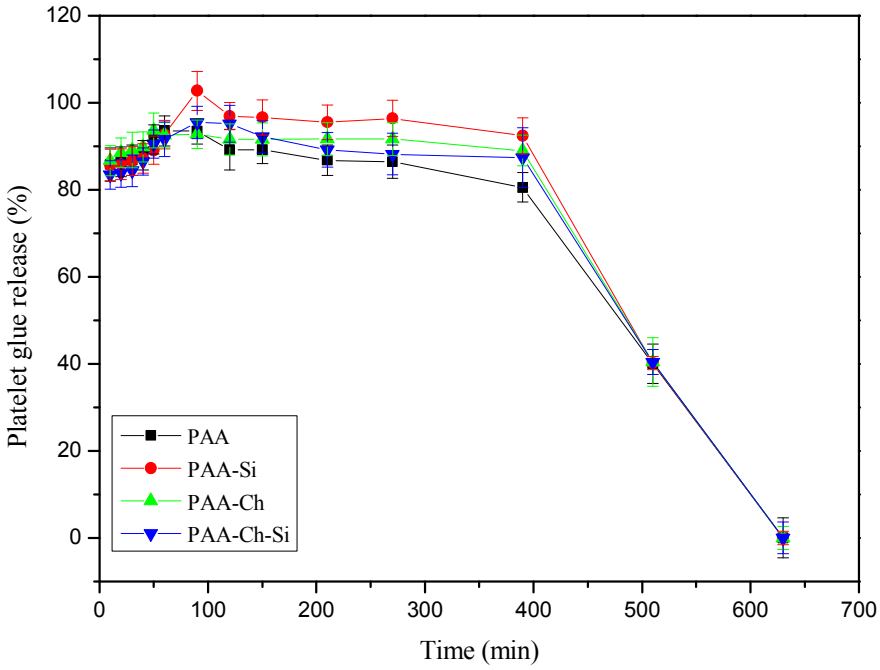

Figure 7. Platelet gel released from hydrogels with different compositions.

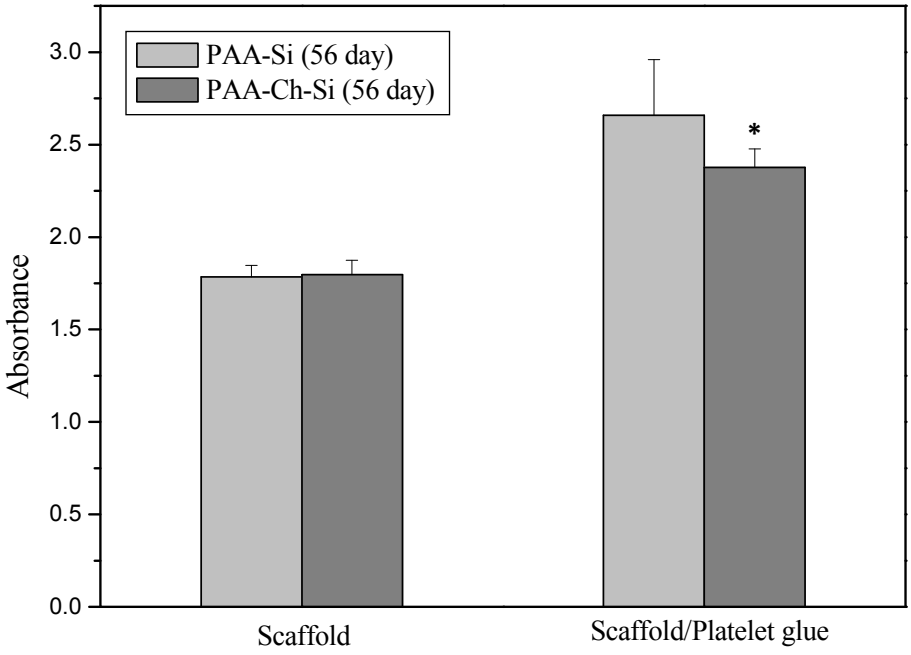

Figure 6. MTS test results of PAA-Si and PAA-Ch-Si hydrogel scaffolds and that added with platelet gel (*$P < 0.05$ as compared PAA-Ch-Si scaffold to PAA-Ch-Si scaffold/Platelet glue).

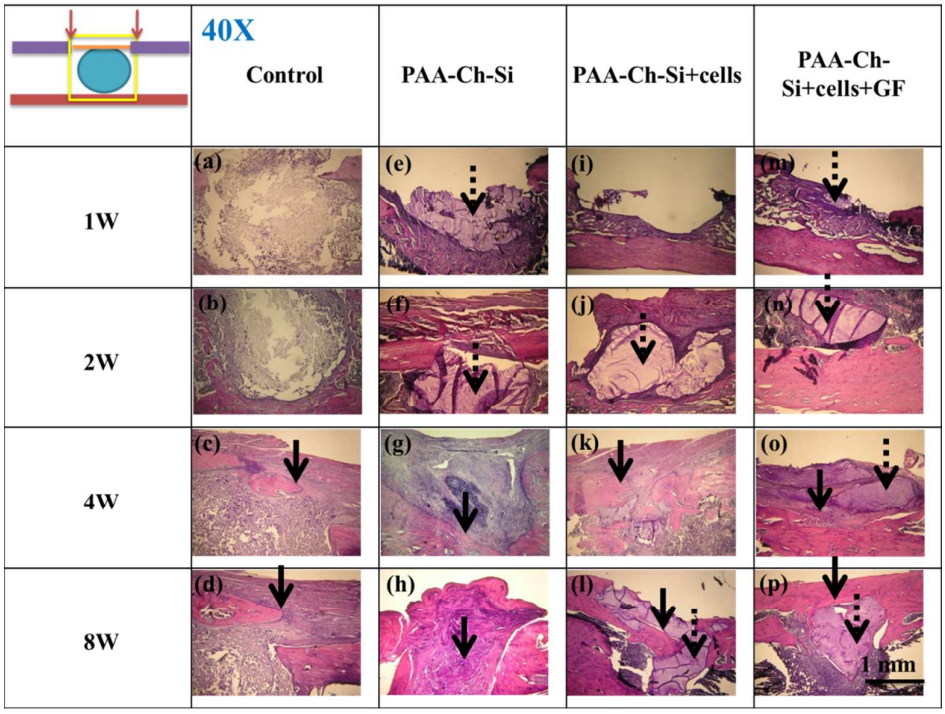

Figure 8. HE stain patterns (40X) of PAA-Ch-Si hydrogel scaffold series observed on different time. The dashed line arrow points the hydrogel, while the solid line arrow points the newly produced bone tissue.

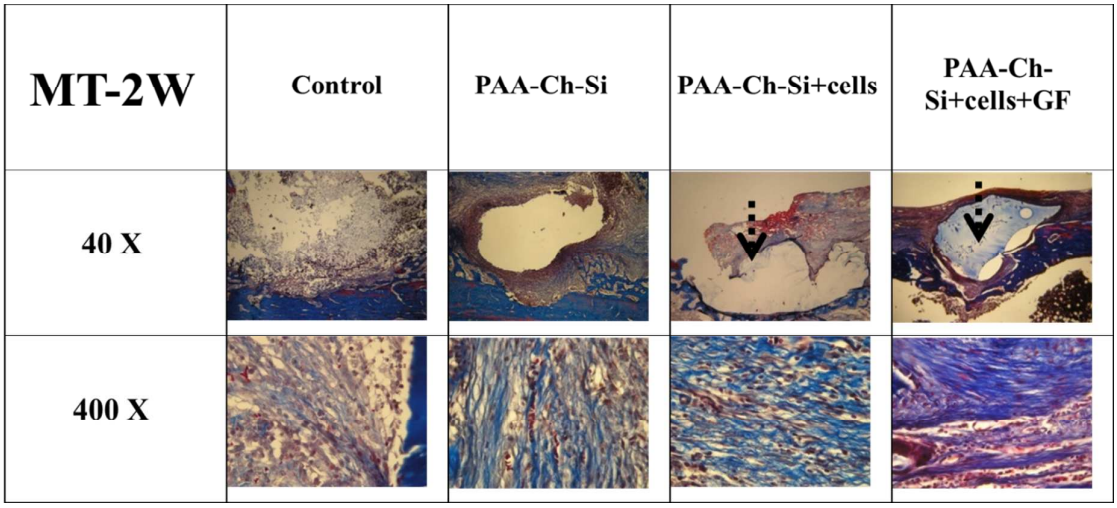

Figure 9. MT stain patterns (40X and 400X) of PAA-Ch-Si hydrogel scaffold series observed in the second week. The dashed line arrow points the hydrogel.

Graphical abstract

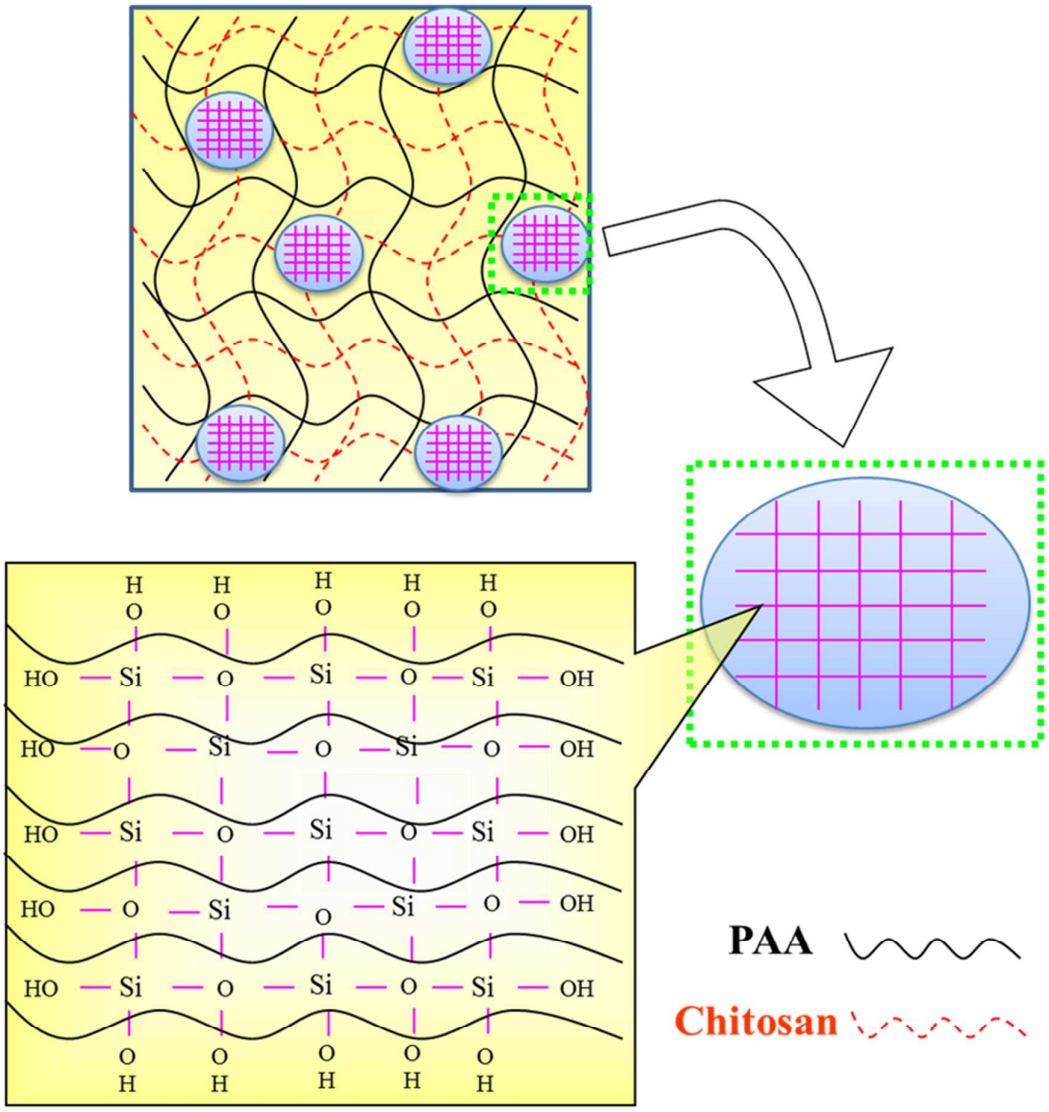

Polymer scaffold with an interpenetrating network (IPN) structure between PAA and chitosan with nano-silica as filler for bone tissue engineering